The dynamical crossover in attractive colloidal systems

Francesco Mallamace,[1,2] Carmelo Corsaro,[1] H. Eugene Stanley,[3] Domenico Mallamace,[4] and Sow-Hsin Chen[2]

[1]*Dipartimento di Fisica e Scienze della Terra, Università di Messina and CNISM, I-98168 Messina, Italy*
[2]*Department of Nuclear Science and Engineering, Massachusetts Institute of Technology, Cambridge, Massachusetts 02139, USA*
[3]*Center for Polymer Studies and Department of Physics, Boston University, Boston, Massachusetts 02215, USA*
[4]*Dipartimento di Scienze dell'Ambiente, della Sicurezza, del Territorio, degli Alimenti e della Salute, Università di Messina, I-98166 Messina, Italy*

We study the dynamical arrest in an adhesive hard-sphere colloidal system. We examine a micellar suspension of the Pluronic-L64 surfactant in the temperature (T) and volume fraction (ϕ) phase diagram. According to mode-coupling theory (MCT), this system is characterized by a cusp-like singularity and two glassy phases: an attractive glass (AG) phase and a repulsive glass (RG) phase. The $T - \phi$ phase diagram of this system as confirmed by a previous series of scattering data also exhibits a Percolation Threshold (PT) line, a reentrant behavior (AG-liquid-RG), and a glass-to-glass transition. The AG phase can be generated out of the liquid phase by using T and ϕ as control parameters. We utilize viscosity and nuclear magnetic resonance (NMR) techniques. NMR data confirm all the characteristic properties of the colloidal system phase diagram and give evidence of the onset of a fractal-like percolating structure at a precise threshold. The MCT scaling laws used to study the shear viscosity as a function of ϕ and T show in both cases a fragile-to-strong liquid glass-forming dynamic crossover (FSC) located near the percolation threshold where the clustering process is fully developed. These results suggest a larger thermodynamic generality for this phenomenon, which is usually studied only as a function of the temperature. We also find that the critical values of the control parameters, coincident with the PT line, define the locus of the FSC. In the region between the FSC and the glass transition lines the system dynamics are dominated by clustering effects. We thus demonstrate that it is possible, using the conceptual framework provided by extended mode-coupling theory, to describe the way a system approaches dynamic arrest, taking into account both cage and hopping effects. © *2013 AIP Publishing LLC*. [http://dx.doi.org/10.1063/1.4833595]

I. INTRODUCTION

Dynamic arrest in condensed matter, i.e., the glass transition, is an intriguing phenomenon that has not been adequately explained.[1,2] This dynamic slowing down process changes system properties and its underlying microscopic origin is a topic of much current research.[3] To study the phenomenon we analyze system transport quantities (e.g., viscosity η, the relaxation time τ, and self-diffusion constant D_s) as functions of thermodynamic variables (e.g., temperature T and concentration C).[4] This approach has received much attention—experimentally, numerically, and theoretically—in the glass-transition literature, but the usual methodology is to explore the T-dependence of these coefficients by supercooling liquids into the metastable state below the melting temperature T_M until they either crystallize or vitrify. Often the concentration (or the volume fraction ϕ) can reveal the control parameter,[5–10] e.g., in complex fluids (supramolecular systems, polymers, colloids, and granular materials).

We can better understand the arrest phenomenon by observing how η, D_s, and τ evolve as a function of the "control parameter" as they approach their limiting values. When $T < T_M$ in supercooled liquids, the transport coefficients change by many orders of magnitude, e.g., often when determining τ the time required for experimental accessibility

is exceeded. These marked changes suggest that we need to determine whether transport parameters reflect an underlying phase transition to a state in which quantities become infinite (a "dynamic divergence" at the calorimetric glass transition temperature T_g).[11,12] Numerous models and theories—many contradicting each other—have been developed to understand the behavior of liquids in their supercooled phase.[4,13–16] A precursor phenomenon exhibiting anomalous ("glassy") dynamics at the transition from liquid to amorphous solid prior to T_g has also been observed. Its evolution is connected to a "critical temperature" $T_c > T_g$. The usual model to describe this is the well-known mode-coupling theory (MCT). An ideal MCT that models density fluctuation dynamics in order to understand the cage effect has been the usual mode of interpreting experimental data inside these temperature regions. MCT utilizes closed equations of motion—in which equilibrium structure enters as input via the static structure factor $S(q)$—for the normalized density-fluctuation correlation functions $F(q, t)$ at wave-vector q.[4] MCT explains T_c for the self-trapping problem of density fluctuations as a singularity that results in a bifurcation phenomenon, and the observables are characterized by two different behaviors above and below T_c. Note that T_c represents a crossover between two different dynamic behaviors located inside the temperature range between

T_M and T_g, i.e., inside the supercooled regime. Above T_c the correlation functions decay to zero according to precise scaling laws (supporting the case for the arrest's universality). Below T_c the interactions of density fluctuations arrest the previous region via cage-effects. The task is to clarify whether in fact the dynamic evolution of the system in the region between T_c and T_g is a crossover due to cage-effects on some kind of activated transport.

MCT describes the measured relaxations of the time-dependent density correlation function by means of two contributions: primary α-processes and secondary β-processes in which molecules explore all the available cage space. In the quasi-elastic scattering (QES) time regime, the two contributions are superimposed, with the β contribution at the lowest time. Both of these contributions obey precise scaling laws.[4] Approaches that are more qualitative than MCT assume that the long time (α-) density correlation function decays of supercooled fluids are caused by the presence of a hierarchical multi-exponential temporal relaxation,[2] observable as a stretched exponential ($F(q, t) = F_q^c \exp[-(t/\tau_\alpha)^{\beta_S}]$). The behavior of the corresponding transport quantities differs from the well-known Arrhenius behavior (AE: $\ln \eta/\eta_0 = E/k_B T$).

Super-Arrhenius (SA) behavior can be variously described using approaches ranging from the power laws typical of the MCT[4] to empirical equations (see, e.g., Ref. 17), such as the Vogel-Fulcher-Tammann (VFT) equation $\eta = \eta_0 \exp(B/(T - T_0))$ in which B and T_0 are material-dependent parameters. Unlike AE, SA predicts a divergence at a finite T_0. The diverging scales of τ, D_s, and η contained in the VFT help us understand the arrested matter process[11, 12] because T_0 is associated with the Kauzmann temperature T_K,[15] i.e., $T_0 \sim T_K$. As an ideal glass temperature, T_K is defined as the temperature at which the configurational entropy S_C of the liquid phase extrapolated below the transition converges with the crystal phase entropy. The Adam-Gibbs theory[12] relates the structural relaxation time, τ_α, to the change in S_C, i.e., $\tau_\alpha = \tau_0 \exp(A/TS_C)$. By considering S_C as $S_C = S_0(T - T_K)/T$ it goes to zero at a finite temperature, hence one obtains the VFT form for which T_K is identified as T_0, and the supports of the VFT physical validity lie in this temperature identification.

Unlike AE behavior in which a single particle hops over barriers of uniform height, in cooperative SA behavior the barriers have a broad distribution of heights, i.e., the so-called inherent structures[18] proposed to describe the thermodynamical behavior of supercooled glass forming liquids. This latter approach is based on the potential energy topology, e.g., the number and depth of local minima (basins) in the potential energy landscape. This picture explains how the system short-time dynamics are characterized as an intrabasin motion and the long-time slow dynamics as an interbasin motion.

A commonly used classification of glass forming liquids identifies two main classes in terms of their "fragility":[19] "fragile" liquids exhibit a marked VFT temperature-dependent behavior and "strong" liquids exhibit a pure Arrhenius dynamic behavior. Whether VFT is a "universal" feature has recently been called into question, e.g., it has been pointed out[20] that $B = D_T T_0$ does not in fact yield the Arrhenius form for $T_0 = 0$.

Another characteristic of supercooling is that microscopic cooperative processes determine the way in which the glass phase is approached.[21–24] Upon cooling, a liquid does not become a glass in a spatially homogeneous fashion. These heterogeneities are regions of space that exhibit strong dynamic correlations such that transport parameters are decoupled leading to the violation of the Stokes-Einstein (SE) relation that occurs at a certain crossover temperature ($T_\times$) with $T_g < T_\times < T_M$. Like T_M, $T_\times$ is a material-dependent property.

From an analysis of the thermal behavior of $\eta(T)$, it has been also conjectured that some supercooled liquids can display a fragile-to-strong (FS) crossover temperature in a region from T_g to T_M located inside the supercooled phase (see Ref. 25 and references therein). An analogous situation has been hypothesized for water at $T_\times \sim 228$ K[26] by assuming that the crossover corresponds to a change in the liquid structure. This was confirmed recently using experimental techniques[27, 28] and molecular dynamic simulations[29, 30] in both confined and bulk supercooled contexts. It was observed that both the SE violation and the dynamic FS crossover take place at the same temperature, $T_\times \sim 225$ K.

Many studies have proposed that transport parameters can exhibit universal features inside the supercooled phase.[14, 25, 31–33] It has also been argued that the microscopic origins of the breakdown of the SE relation and of the dynamic FS crossover lie in the dynamic heterogeneities. In the vast literature on the topic, the scaling laws typically used to describe critical phenomena and the physics of complex materials such as polymers and gels have been not very used to describe dynamic arrest. The VFT approach has been used instead,[34] despite the fact that there are many new studies and ideas now available on dynamic arrest.

In addition to the question of whether a true "diverging behavior" in the dynamic parameters exists, we also want to determine the liquid-to-glass transition temperature. In terms of viscosity and relaxation times, there is no precise T_g, only a transformation region—and the resulting glass is in a high-viscosity supercooled liquid state. In terms of these parameters there is no distinction between the glassy and the supercooled liquid states. Neither T_0 nor T_g appears relevant in describing and understanding their slowing down. Note that in this scenario the VFT approach lacks physical meaning. This is related to the observation, made in some statistical mechanics studies, that the configurational entropy is finite at any temperature,[16] i.e., a Kauzmann temperature T_K, where the liquid is out of the equilibrium, does not exist. A study[33] of the dielectric relaxation times $\tau(T)$ of many ultraviscous glass-forming fluids contradicts the VFT prediction that transport parameters diverge at a finite T and demonstrates that the VFT cannot explain supercooled liquid dynamics. The dominant position of VFT has also been questioned by other authors,[17, 35] and the superiority of several equations for showing no-divergence at a finite T proposed. This scenario was confirmed in terms of the segmental relaxation data of glass-forming polymers as $T \to T_0$[36] where the time scales related to the arrest do not diverge at a non-zero temperature. Divergent vs. non-divergent dynamics has recently received extensive study, and new light has been shed on the behavior of

supercooled systems and a new relationship between the glass transition and critical phenomena revealed.[37]

These observations in both small glass-forming molecules and polymers suggest a larger generality, which is confirmed by the dynamic crossover caused by the universal behavior of transport parameters and not by a definition linked to a specific cooling rate, such as the calorimetric T_g.[38] In the fractional SE (the scaled representation of the transport parameter) data of many different supercooled liquids converge into a single master curve (Figure 3 of Ref. 38) and their decoupling takes place at $T_\times$ where the system reverts to AE behavior.

As stated above, MCT has been used to determine the temperature at which fragile supercooled liquids below T_M undergo dynamic changes,[14,25,31,32,35,39,40] an approach confirmed by a recent study of the critical behavior of glass forming liquids.[37] It has also been proposed that the FS crossover temperature can be identified as the critical temperature of the ideal MCT T_c (hence $T_\times = T_c$), suggesting that an extended MCT (EMCT) can be used to describe the entire FS scenario.[41,42] We can thus use a MCT power law form to determine the transport parameters,

$$\eta = \eta_0 \left| (T - T_c)/T_c \right|^{-\gamma}, \quad (1)$$

where γ is a non-universal exponent. Although the ideal MCT assumes that structural relaxation is the bottleneck for all molecular motion, the EMCT suggests that phonon-assisted hopping processes can fully explain structural relaxation processes.[41] Even if the SA region can be described by its original formulation[4] (which also introduced the concept of crossover temperature), the entire temperature behavior of the transport parameters, above and below the dynamical crossover, is better described using an extended form that incorporates barrier hopping.[42] The main observations are that[43] $T_c = T_\times$ appears to be more relevant than T_g or T_0 to the physics of the dynamic arrest, and the universality shown in the master curves from the scaled description of the Stokes-Einstein and Debye-Stokes-Einstein violations is a "ground-breaking" reality that suggests a new approach to exploring arrested processes. Our work demonstrates that MCT can be used to form a comprehensive description of this phenomenon.

We use the viscosity data of an attractive colloidal system characterized by a well-defined clustering process to confirm that the dynamic crossover $T_c = T_\times$ through transport data indicates the presence of dynamic arrest. We do this to prove that using the extended MCT based on hopping processes is valid and to point out that using system concentration as a control parameter further supports the proposed universality of the arrest process, i.e., the goal of this work is to prove that the fragile-to-strong (FSC) can also be observed by changing the concentration of the system (or its compressibility). Hence, the behavior of a colloidal system is the same as that of a molecular supercooled liquid. This unique approach to understanding dynamic arrest utilizes the vast previous research on colloids and polymers and the technique of interpreting transport parameter evolution as a function of concentration.

We note that the hard-sphere system (HS) has been used as a theoretical paradigm for a simple fluid and that experiments conducted on HS colloids indicate that it can also serve as an accurate test of models developed to explain glass dynamics.[5–7] Originally, it appeared that the ideal glass transition concentration of the MCT was identical to the "calorimetric" glass transition, $\phi_c = \phi_g$. This suggests that studies of colloidal systems can help us understand the conventional glass transition, which is usually studied in molecular liquids. Recently, attractive colloids (polymer grafted colloids) and an adhesive hard-sphere system (AHS—block-copolymer micelles) were also considered. Unlike the previous systems (HS and molecular liquids) in which the MCT bifurcation is due to changes in a single control parameter (fold bifurcation), in the case of attractive systems there is a possible cusp bifurcation, i.e., a MCT singularity obtained when two control parameters are varied. This type of bifurcation differs completely from folding in the sense that it causes, even in the liquid region, a logarithmic decay in the correlations. Specifically, these AHS systems are characterized by two intersecting glass-transition lines in the $T - \phi$ phase diagram, indicating the hard core and the adhesive part of the potential, respectively, and giving rise to two different arrest mechanisms.[8] This scenario was fully confirmed in a number of colloidal materials[44] and suggests that we can observe the arrest by changing the volume fraction and the temperature. By changing the temperature the liquid can become a glass both on cooling and on heating.[45] Note that in these AHS colloids an A3 singularity point at which the glass-to-glass transition line terminates can occur. MCT suggests that the two distinct dynamically arrested states become identical at and beyond this singularity point.[8,9]

We next examine viscosity data from the AHS copolymer micellar system, which indicate the presence of a MCT cusp bifurcation.[9,46] Using T and ϕ as control parameters we study the FS dynamic crossover and show that the extended form of the MCT can aptly describe the corresponding behaviors. These transport quantities came from viscosity experiments.[47–49] Note that the nuclear magnetic resonance (NMR) technique[50] provides evidence for a clustering process caused by interparticle attraction. This process is the basis of the cusp singularity that determines the physics of this complex system.

II. CURRENT STATE-OF-THE-ART

In quasi-elastic light scattering (QES) the two MCT temporal contributions are superimposed with the β-contribution at the lowest time. In the frequency dielectric spectra the β-contribution is located at a frequency above that of the α-peak ($\omega_\alpha = 1/\tau_\alpha$). In the β relaxation, we can describe the extracted relaxation times by using activated AE T behavior $\ln \tau_\beta/\tau_{\beta 0} = E(T)/k_B T$, in contrast to τ_α, which exhibits SA behavior. These data from two time scales indicate the existence of a crossover temperature T_c located above T_g at which the dynamic behavior of the system evolves from that typical of a strongly coupled fluid to that of a glass. Near T_c the α-relaxation governing the long-time fluid dynamics characterized by a power law behavior and anomalies in the Debye-Waller factor exhibits a stretched exponential form.[4]

The β-process has its onset at the crossover, whereas the α-contribution reveals it with two fractal time-decay behaviors (with non-universal exponents). Short times produce identical dynamics from both the fluid and glass sides, while long times produce saturating correlation functions in the glass phase.

Hence, the ideal MCT crossover temperature can be measured using the two time scales and the α-process in terms of the form [Eq. (1)], $\tau_\alpha = \tau_{\alpha0}|(T - T_c)/T_c|^{-\gamma}$. This power law describes the transport properties only in the region $T_M > T > T_c$, and thus in the T-range from the stable liquid phase to the supercooled phase.[4] Power law approaches have been also used, independent of the MCT, to describe the thermal transport parameter behavior that occurs as a normal liquid enters the moderately supercooled region when T is lowered.[5,25,31,32]

The MCT indicates that the glassy relaxation originates in the fold bifurcation of the long-t limit of the normalized density correlator. This limit, zero in the liquid phase and positive in the ideal glass, is called the non-ergodicity parameter or the Debye-Waller factor f_q. It is discontinuous if the control parameter passes some critical value (e.g., ϕ_c or T_c). Hence, f_q exhibits a singularity as a function of the distance $\epsilon = (T - T_c)/T_c = (\phi - \phi_c)/\phi_c$ for $\epsilon = 0$. Designating $\sigma = C\epsilon$, the separation parameter, the β-relaxation scale is derived from $t_\sigma = t_0/|\sigma|^{1/2a}$ (with the exponent $1/2a > 1.27$). In the second scaling law regime (α-), the ideal MCT again gives a power-law divergence but the γ exponent is larger than that of t_σ ($1/2a$), i.e., $\tau_\alpha = B^{-1/b}t_0|\sigma|^{-\gamma}$ and $\gamma = [1/(2a) + 1/(2b)]$. The anomalous exponents $0 < a \leq a_{\max} = 0.395$ (i.e., the critical exponents) and $0 < b \leq 1$ are related through the system-dependent exponent parameter λ ($1/2 \leq \lambda < 1$) via $\lambda = \Gamma(1 - a)^2/\Gamma(1 - 2a) = \Gamma(1 + b)^2/\Gamma(1 + 2b)$. A study of the dynamic parameters performed in a polymer or colloidal solution as a function of the volume fraction ϕ has confirmed these MCT suggestions. QES experiments made in hard-sphere colloids for $\phi < \phi_c$, which measure both the self-diffusion coefficient D_s and τ_α, fully support these suggestions, giving $\gamma = 2.7$.[6] In polystyrene-networked-sphere colloids, however, $\gamma = 3.6$ and $\lambda = 0.88$.[51]

The EMCT predicts a dynamic crossover in τ_α and in D_s. The crossover occurs near the ideal T_c and is due to the dynamic change in the system from one determined by the cage effect to one characterized by the hopping processes. The crossover is a FS crossover in which the α-relaxation time and the self-diffusion undergo a crossover from SA to AE behavior. This result, obtained for a Lennard-Jones system, explains the FS crossover observed in a variety of glass-forming fluids.[41,42] This EMCT approach also demonstrates that the SE relation breaks down in different ways on the fragile and strong sides of the FS crossover, in agreement with experimental observations of confined water[28] and liquid $Pd_{43}Cu_{27}Ni_{10}P_{20}$ alloys.[52]

Specifically, in EMCT terms, the scale decoupling for $T < T_c$ is explained by assuming that the relaxation is due to thermally activated hopping processes. The self-diffusion coefficient (like the other transport parameters) is thus $D_s \approx D^{\text{hop}} + D^{\text{id}}$, with the dynamic crossover at $T \approx T_c$ from $D \approx D^{\text{id}}$ to D^{hop}. The EMCT numerical results[41] show that the ideal contribution D^{id} vanishes at $T_c/T = 1$ with a power law $D^{\text{id}} \sim |T - T_c|^\gamma$, according to the dynamical arrest behavior predicted by the idealized theory. Hence, for $T < T_c$ the behavior of D_s is determined only by D^{hop}. In addition, at these low temperatures the self-diffusion coefficient exhibits AE behavior.

The MCT power law fits the transport parameter data in the SA region and indicates the temperature point ($T_\times \equiv T_c$) at which the experimental data cross that of the Arrhenius behavior. This EMCT analysis indicates the physical significance of the concept of T_c in terms of a well-established theory of glass-forming systems, rather than of numerous empirical observations. The FS and the SE both occur at T_c, for which $T_\times \equiv T_c$. This was confirmed by the ideal MCT used to study the viscosity of many different supercooled liquids that used T as the control parameter and evaluated the corresponding T_c and the γ exponent.[43]

We also see FS crossover when we make the volume fraction ϕ the control parameter, and ϕ_c, like T_c, is the separation between the two different dynamics. To account for this, we have considered a copolymer micellar system in which the short-range attraction is due to an effective intermicellar interaction. The system is an aqueous solution of a nonionic, three-block copolymer made of polyethylene and polypropylene oxides (Pluronic L64). This polymer in water is a T-dependent surfactant that forms monodisperse spherical micelles in a wide $T - \phi$ range. The system, widely described in many experiments,[9,46–49,53,54] presents a very rich phase diagram (see Fig. 1). Because of intermicellar interaction there is an inverted binodal line with a lower consolute critical point, a $T - \phi$ dependent percolation line separating a liquid-like from a gel-like phase and, as predicted by the MCT, a glassy line. Because it is a system with a hard core and an additional short-range attractive interaction (i.e., an AHS system), a special arrest scenario characterized by cusp singularity emerges. In addition to particle packing ϕ (used for HS colloids to describe the fold singularity), the temperature serves as a second external control parameter. The system is thus characterized by a reentrant liquid-to-glass transition with two liquid-glass transition lines.[8] At high T and sufficiently high ϕ, the system evolves into the well-known "repulsive" glassy state. At relatively low T, however, an "attractive glass" forms and the particle motion is hindered by clustering. We, thus, divide spherical colloidal systems into two categories: (i) a one-length-scale hard-sphere system in which glass formation is dictated by the cage effect and (ii) a two-length-scale AHS with a second glass-forming mechanism: a clustering process caused by interparticle attraction.

III. METHODS

A. Sample

We prepare the micellar system by dissolving a triblock copolymer PL64, a member of the Pluronic (BASF AG, Ludwigshafen, Germany) family that is used extensively in industrial applications, into D_2O at different weight fractions C. Pluronic is a combination of polyethylene oxide (PEO) and polypropylene oxide (PPO). The chemical formula of L64 is $(PEO)_{13}(PPO)_{30}(PEO)_{13}$ and it has a mass of 2990 Da.
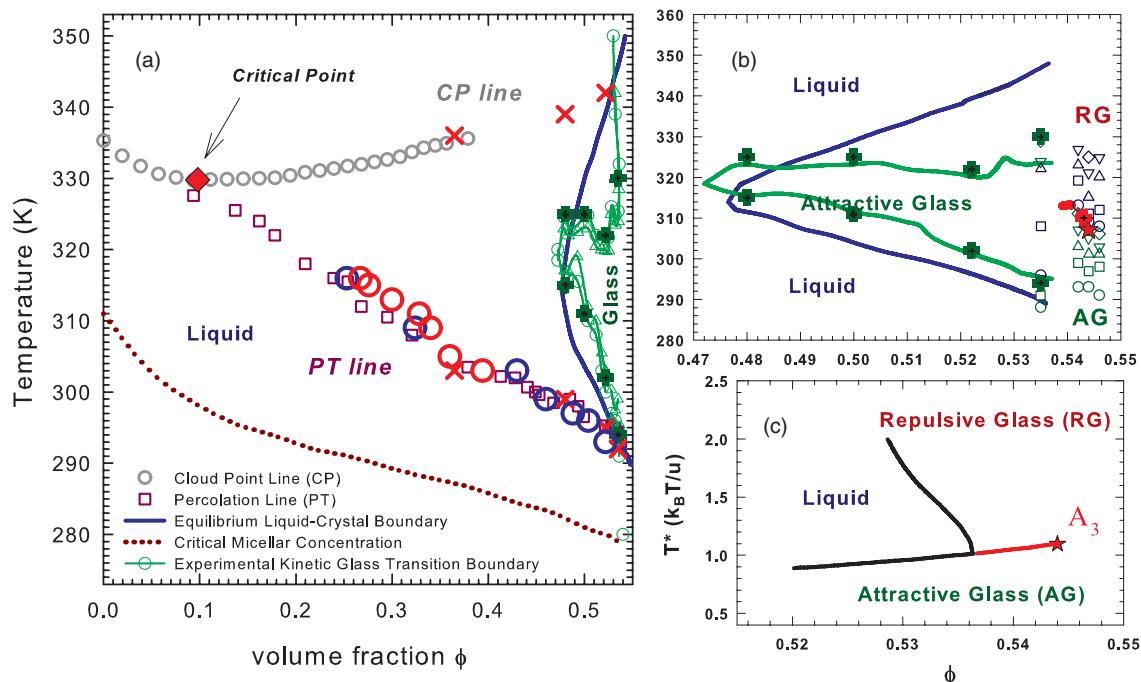
FIG. 1. (a) The experimental $T - \phi$ phase diagram for the adhesive hard sphere (AHS) system PL64/D$_2$O characterized by an inverted binodal, CP, line with the critical point (cloud point line, CP), the critical micellar concentration line (CMC), and a percolation line.[9,49] Are also indicated the equilibrium phase boundary between the disordered micellar phase and the ordered liquid crystalline hexagonal phase (blue line)[55] and an experimentally obtained (lights and neutron scattering) kinetic glass transition line in the ranges $0.47 < \phi < 0.55$ and $288 < T < 353$ K (green lines and symbols). Large symbols correspond to the NMR (red × and green crosses) and viscosity data (large blue and red circles obtained by using T and ϕ as the control parameter, respectively) of the present work. (b) Details of the experimental phase diagram, in the ranges $0.47 < \phi < 0.55$ and $280 < T < 360$ K, (open symbols)[9,53,54] reporting the equilibrium phase boundary and, in green the glass transition line (liquid-attractive glass). This figure also illustrates the transition between two distinct amorphous states (attractive AG and repulsive RG, respectively) in the interval $0.536 < \phi < 0.544$ (open symbols deal with experimental observations, green for the AG and blue for the RG). (c) The theoretical phase diagram (T^* vs. ϕ) predicted by MCT calculations for the case of $\Theta = 0.03$ (attractive well width). It can be observed the cusp like singularity typical of AHS materials,[4,8] the glass-liquid-glass re-entrant behavior and an attractive-to-repulsive glass transition line starting where the two branches cross and terminate at A_3 [$\phi(A_3) = 0.544$], beyond which the long-time dynamics of two glassy states become identical. In (b) and (c) the red star identifies the A_3 singularity.

Because PEO and PPO are hydrophilic at low temperatures, L64 chains readily dissolve in water and exist as unimers. As the temperature increases, the hydrogen-bond formation between water and polymer molecules decreases, PPO becoming less hydrophilic more rapidly than PEO, and the copolymers acquire surfactant properties and aggregate to form micelles. Because at higher temperatures water becomes a progressively poorer solvent for both PPO and PEO chains, the inter-micellar interaction becomes attractive (the system behaves like a grafted colloid). The evidence for the increased short-range micellar attraction as a function of T comes from the existence of a critical point at $C \simeq 0.05$ and $T = 330.9$ K and a percolation line. Theoretically,[8,44] the phase behavior of the micellar system is characterized by an effective temperature $T^* = k_B T/u$, the volume fraction of the micelles ϕ, and the fractional attractive well width $\Theta = \Delta/d$, where k_B is the Boltzmann constant, $-u$ is the depth of the attractive square well, Δ is the width of the well, and d is the diameter of the hard core. Hence, for a given Θ, aside from ϕ, as in the case of a pure hard sphere system, the effective temperature T^* is introduced into the description of the phase behavior of the system as a second external control parameter and thus the loss of ergodicity can take place by increasing either ϕ or T^*. Neutron scattering experiments have been used to evaluate T^* as a function of the normal temperature T at different

ϕ[53] showing that, as T increases, T^* also increases. By measuring the micellar aggregation number N as a function of T at different ϕ, the same experiments showed that the degree of self-association increases as T increases at a given ϕ. This is consistent with the fact that the PPO core becomes less hydrophilic at higher temperatures. In addition, at a given temperature, N decreases as ϕ increases—a behavior indicating that u increases as ϕ increases. Furthermore, by comparing the effective temperatures obtained from fitting the experimental data in the liquid and glass states, it can be seen that the depth of the square well increases as T and ϕ increase, making a liquid-glass transition possible.

Figure 1(a) shows the experimental $T - \phi$ phase diagram of an AHS PL64/D$_2$O system.[9,49] Note that it is characterized by an inverted binodal line with a critical point (cloud point line CP) and a percolation line. We choose heavy water so that we can compare the neutron data with those from other experimental techniques. Figure 1(a) also shows the critical micellar concentration (CMC) line, the equilibrium phase boundary (blue line) between the disordered micellar phase and the ordered liquid crystalline (hexagonal) phase[55] and, using light and neutron scattering,[9,53] an experimentally obtained glass line in the ranges $0.47 < \phi < 0.55$ and $288 < T < 353$ K (green line and open green symbols). Figure 1(b) shows the phase diagram in the ranges $0.47 < \phi < 0.55$ and

$280 < T < 360$ K and combines the equilibrium phase boundary, the kinetic glass transition line (liquid-attractive glass), and the transition between two distinct amorphous states (attractive (AG) and repulsive (RG) glasses, respectively) within the volume fraction range from 0.536 to 0.544 (with open symbols for experimental observations, green for the AG, and blue for the RG). Note that the amorphous states in this region of phase space are metastable states of the system, e.g., as in supercooled liquids. In summary, in this AHS system the liquid glass transition line is a function of both ϕ and T.

Figure 1(c) shows the theoretical phase diagram (T^* vs. ϕ) predicted by MCT calculations for the case of $\Theta = 0.03$ (the attractive well width). Due to the competition between cage and clustering processes a reachable phase diagram appears that, depending on the control parameters used, is characterized by a liquid region and two kinetic glass transition lines, one corresponding to the HS glass at high composition (the repulsive branch) and the other extending into much lower concentrations (the attractive branch). MCT attributes the repulsive branch (with the usual packing effect) to the repulsive interaction and the attractive branch to the attractive region of the potential. Figure 1(c) shows a cusp-like singularity exhibiting glass-liquid-glass re-entrant behavior and an attractive-to-repulsive glass transition line beginning where the two branches cross and terminating at A_3 [$\phi(A_3) = 0.544$], beyond which the long-time dynamics of the two glassy states become identical. In Figs. 1(b) and 1(c) the red star indicates the A_3 singularity point.

We study the result as a function of both control parameters, T and ϕ, in order to clarify the arrest properties of a system dominated by a clustering process caused by attractive interaction, and carry out a series of NMR and viscosity (η) experiments in the AHS PL64/D_2O system. In particular, we consider the zero shear viscosity measured at several different concentrations in the range $0.096 < \phi < 0.537$ as a function of T. From these data we observe that, starting from low T, η increases steeply, first going through a percolation transition and then a liquid-to-glass transition. When $\phi < 0.4$ there is only a percolation transition, and the dynamical arrest is only in the region of the crystalline hexagonal phase.

B. Experiments

The NMR experiments are carried out using a spectrometer operating at 700 MHz ^1H resonance frequency (Bruker AVANCE). The system dynamics are measured using the Pulsed Gradient Spin-Echo technique (^1H-PGSE)[56] in the 288–343 K temperature range in the $0.15 < \phi < 0.547$ interval (the T-dependence of the methanol chemical shift is used as a T standard). The details of the NMR experiment are reported in Ref. 57. We derive the mean square displacement $\langle r^2(t) \rangle$ of the Pluronic L64 molecules diffusing in the NMR pulsed-field gradients direction r, during the time interval t. Hence, we study the micellar dynamics by examining the proton NMR relaxation.

We measure the viscosity in identical systems and under identical experimental conditions using a strain-controlled rheometer with double-wall Couette geometry at a fixed fre-

quency $\omega = 1\,s^{-1}$ under conditions that ensure a linear response where clustering processes originate. We increase the viscosity by varying both control parameters, a response due to the clustering process associated with the percolation transition.[9,49,54] Note that both the loss module $G'(\omega)$ and storage module $G''(\omega)$ are frequency-dependent. According to theory,[34] near the percolation threshold these moduli exhibit a precise universal scaling behavior with G'' dominant over G': $G' \approx G'' \approx \omega^k$, k being a universal exponent with an expected value of 0.7.[47]

By measuring the mean square displacement (MSD) $\langle r^2(t) \rangle$ of the molecules (or the MSD of their protons) in a given time interval, the NMR method adopted here has been widely used to study the self-diffusion process in polymer systems. This approach takes into account the fact that complex materials, such as those dominated by aggregation and clustering, can exhibit generalized Brownian motion (i.e., Lévy flight or fractal diffusion) rather than simple Brownian motion.[58] It is well-known that in Brownian motion $\langle r^2(t) \rangle = 2D_s t$, but in fractal diffusion $\langle r^2(t) \rangle \sim t^\alpha$. Homogeneous media have uncorrelated molecular displacements with random thermal motion, but when a hierarchically intricate structure is present, e.g., the self-similar aggregates or clusters of the copolymer, the system dynamics are strongly correlated in both spatial and time scales, giving rise to the power-law behavior between the time and the mean square displacement. For fractal diffusion, $\alpha < 1$, and in the random walk fractal dimension $d_f > 2$, $\alpha = 2/d_f$. We use the PGSE NMR technique to determine D_s and label the nuclear spins using the Larmor precession frequencies in a spatially varying magnetic field. In these experiments we apply a field gradient pulse of magnitude g and find that the spin-echo attenuation ψ is related to the spin self-correlation function $P_S(r|r', \Delta)$, as

$$\psi(\Delta) = \int \rho(r) \int P_S(r|r', \Delta) \exp[i\gamma\delta g(r' - r)dr'dr],$$

where γ represents the gyromagnetic ratio of the nucleus, and Δ and δ are the separation (the observation time) and the width of the gradient pulses, respectively. In the case of nuclei in pure random Brownian motion, the self-correlation function has a simple Gaussian form that, under the narrow pulse width approximation ($\delta \ll \Delta$), is

$$\psi(\Delta) = \exp[-(1/2)\gamma^2\delta^2 g^2\langle r^2(t) \rangle] = \exp[-Q^2 D_s \Delta].$$

Here $Q = (\gamma\delta g)$ is the "NMR generalized" scattering vector.

Figure 2 shows the measured spin-echo attenuation, normalized to its $Q^2\Delta = 0$ value (i.e., ψ/ψ_0 vs $Q^2\Delta$, at different observation and gradient pulse times) for the PL64/D_2O solution with $\phi = 0.485$ at temperatures 288 K and 322 K, below and above the percolation line, respectively. Note that the two spectra are different (especially at larger $Q^2\Delta$), and the single exponential time decay in the spectrum for $T = 322$ K exhibits a more complex behavior, one that corresponds to simple Brownian motion. The inset shows ψ/ψ_0 in a scaled plot. The normalized spin-echo attenuation is a function of the scaling variable $(Q^2\Delta)^\beta$ with $\beta \simeq 0.43$. Within experimental error, this plots the data in a straight line, demonstrating that the spin echo attenuation is a stretched exponential.
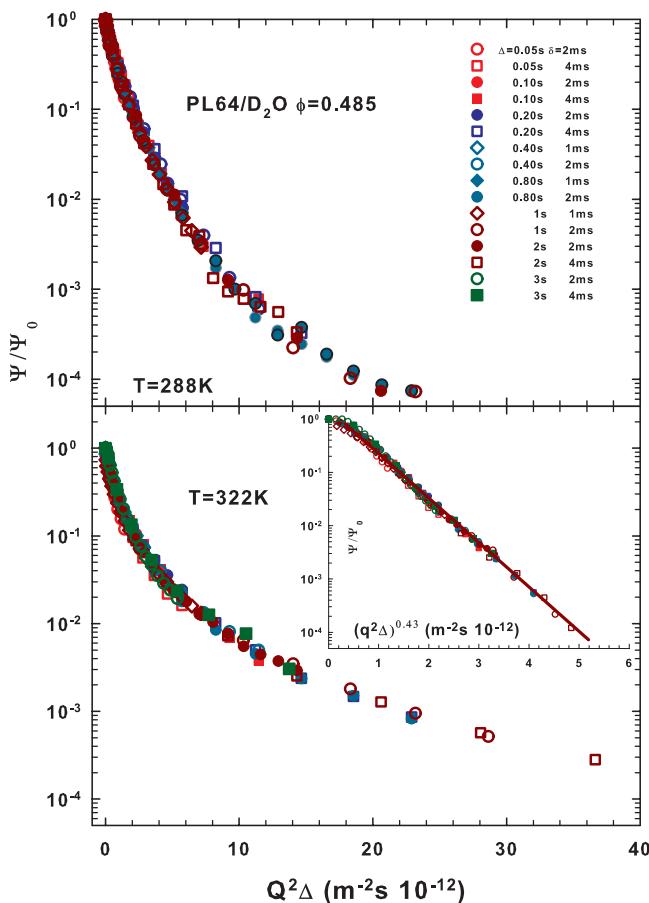
FIG. 2. The normalized pulsed gradient spin-echo NMR attenuation ψ/ψ_0 vs $Q^2\Delta$ (at different Δ and gradient pulse width δ), for the PL64/D$_2$O solution with $\phi = 0.485$ at the temperatures 288 K and 322 K, i.e., below and above the percolation line, respectively. The inset illustrates ψ/ψ_0 data corresponding to 322 K, in a scaled plot; the normalized spin-echo attenuation is reported as a function of the scaling variable $(Q^2\Delta)^\beta$ with $\beta \simeq 0.43$ demonstrating a stretched exponential "character" of the spin echo attenuation.

In NMR experiments the maximum Q value is on the order of 10^7m^{-1}. The experiments thus probe length scales L ($\sim 1/Q$) comparable to those of light scattering (hundreds of nm) rather than of neutrons or X-ray scattering where the characteristic probe length is of the molecular order. Self-similar systems (or percolating networks) are identified by a typical length scale ξ, related to the average cluster size or length scale up to which the cluster can be identified as a fractal. On this basis, the quantities $Q\xi$ or ξ/L identify the system dynamics. $Q\xi$ identifies a crossover between two extreme dynamic regimes, the Porod $Q\xi \gg 1$ regime and the Guinnier $Q\xi \ll 1$ regime. In the Porod regime the technique characterized by $\xi/L \gg 1$ yields details about the intracluster dynamics. On approaching the percolation threshold, a typical NMR experiment can thus satisfy this latter condition and can test the anomalous diffusion,

$$\psi(\Delta) = \exp[-(1/2)Q^2\langle r^2(t)\rangle] = \exp[-Q^2 D_s \Delta^\alpha]$$
$$= \exp[-Q^2 D_s \Delta^{2/d_f}]. \qquad (2)$$

The theoretical percolation models predict $3 < d_f < 4,$[59,60] but at the percolation threshold experiments measure a value $d_f \simeq 4.2.$[61] An NMR study in Pluronic F68 at a concentration of 35 wt. % shows that the exponent α decreases on approaching gelation with a value of ≈ 0.5 inside the gel phase.[50]

We perform numerous NMR experiments inside the crystalline hexagonal phase by approaching from the liquid side and heating the sample at a given volume fraction. Under these conditions the system remains a metastable liquid (supercooled and glass-forming) for times on the order of several hours prior to irreversible crystallization. This is a time longer than the NMR experimental time (≈ 20 min) required to accurately measure the spin-echo attenuation $\psi(\Delta)$, from which we evaluate the exponent α. To keep the metastable liquid from crystallizing, we remove the samples from the NMR spectrometer after each experiment performed at temperatures inside the hexagonal phase and store them in a thermostatic bath at a typical liquid phase temperature (287 K).

IV. RESULTS AND DISCUSSION

A. NMR

Figure 3 shows a log-log scale of the NMR time evolution $\langle r^2(t)\rangle$ for the PL64/D$_2$O system at $\phi = 0.46$ when we change T from 293 K to 333 K. Here $\phi = 0.46$ is a volume fraction in which the micellar system is in the stable liquid
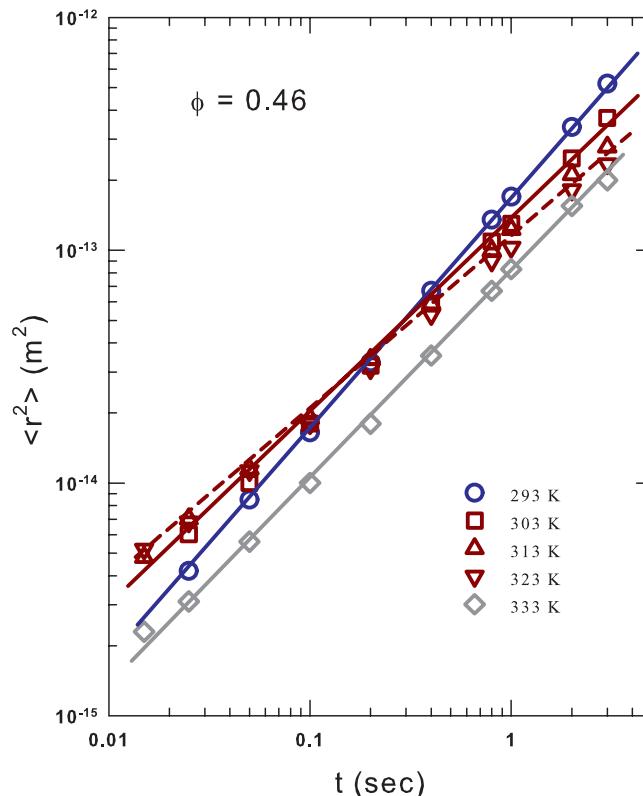

FIG. 3. The plot in a log-log scale of the time evolution of the NMR measured $\langle r^2(t)\rangle$ at different temperatures T ($293 < T < 333$ K) in the copolymer stable micellar phase for $\phi = 0.46$. It is evidenced that when T increases the fractal diffusion exponent, $\alpha(T)$, decreases from 1 to about 0.6 on crossing the percolation threshold (~ 300 K) after that decreases again inside the gel phase and returns to values typical of the pure Brownian diffusion on approaching the cloud point line. The general trend that α decreases during the percolation process is a result of the clustering process that reduces the micellar mobility.
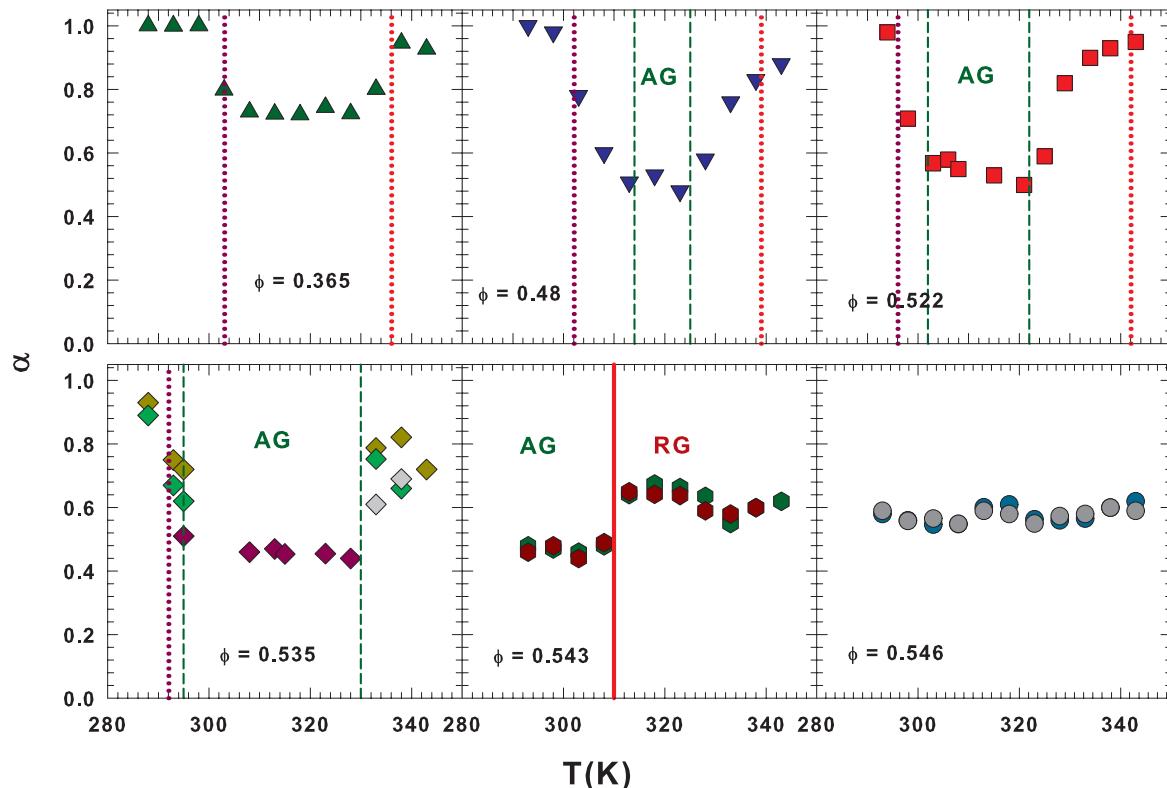
FIG. 4. The T behavior of the fractal exponent $\alpha(T)$ for several different volume fractions in the interval $0.365 < \phi < 0.546$, covering all the complex phase diagram characterized by the liquid, the gel, the attractive glass (AG), and also the high-ϕ area where the system shows the complex situation characterized by the MCT cusp singularity and the glass-to-glass transition.

phase throughout this T range, and the MSD is calculated using Eq. (2) during the gelation process and inside the gel phase. Note that by increasing T above 293 K (just inside the disordered liquid region) the fractal diffusion exponent $\alpha(T)$ decreases from 1 to ≈ 0.6 on crossing the percolation threshold at ≈ 300 K and then decreases again inside the solid-like gel phase and, as it approaches the cloud point line, returns to values typical of pure Brownian diffusion. Hence, the general trend is that α decreases during the gelation, a result of the clustering process in which the micellar mobility is reduced. Figure 4 shows the temperature behavior of the fractal exponent $\alpha(T)$ for several volume fractions of the PL64/D$_2$O AHS system in the $0.365 < \phi < 0.546$ range. It covers the entire complex phase diagram including the liquid, the gel, the AG, and the high-ϕ area where the system exhibits the complex MCT cusp singularity and the glass-to-glass transition. We see significant changes occurring in all areas of the system. When $\phi = 0.365$, the exponent α decreases at $\alpha \sim 0.66$ near the percolation threshold temperature where the characteristic incipient spanning cluster is formed (dotted pink line). At $\alpha \sim 1$ it returns to the cloud point line (dotted red line). Figure 1(a) shows that these crossover temperatures (red ×s) are approximately coincident with both the experimental PT and CP curves. When $\phi = 0.48, 0.522,$ and 0.535 the situation is more complex. In addition to the α changes at the PT and CP temperatures (red ×s), there are two significant changes in the fractal diffusion exponent, (i) one that reduces the exponent value at ~ 0.5 and (ii) one in which the previous higher values are restored. These crossover temperatures

[dashed green lines in Fig. 4 and green crosses in Figs. 1(a) and 1(b)] are nearly coincident with the experimental attractive glass line observed by means of light and neutron scattering experiments.[9,49] This has been confirmed by a MD study on a model system for interacting colloids.[62] From these results it is clear that the $\alpha(T, \phi)$ reproduces well the MCT phase diagram predicted for AHS systems. This is confirmed by the behavior of the α exponent inside the glass-to-glass transition just below ($\phi = 0.543$) and above ($\phi = 0.546$) the singularity point A_3 ($\phi = 0.544$). When $\phi = 0.543$, the exponent value increases from $\alpha \sim 0.42$ to $\alpha \sim 0.6$ at the temperature (red line) where the scattering observations [see Fig. 1(b)] indicate the locus of the system transition from the AG to the RG. When $\phi = 0.546$ (above the singularity point) the exponent behavior is nearly constant throughout the temperature range, i.e., only a glass phase exists.

B. Viscosity

Figures 5 and 6 show the viscosities of the PL64/D$_2$O inside the $\phi - T$ phase diagram when ϕ is fixed as a function of temperature (Fig. 5) and vice-versa (Fig. 6), together with a corresponding MCT data analysis that uses, respectively, T and ϕ as the control parameter. Figure 5 shows a log-linear plot of the viscosities of pure water (red dots) and of the micellar system at volume fractions $\phi = 0.096, 0.181, 0.256, 0.324, 0.43, 0.46, 0.488, 0.504,$ and 0.522 as a function of $1/T$. The open symbols indicate the behavior of the
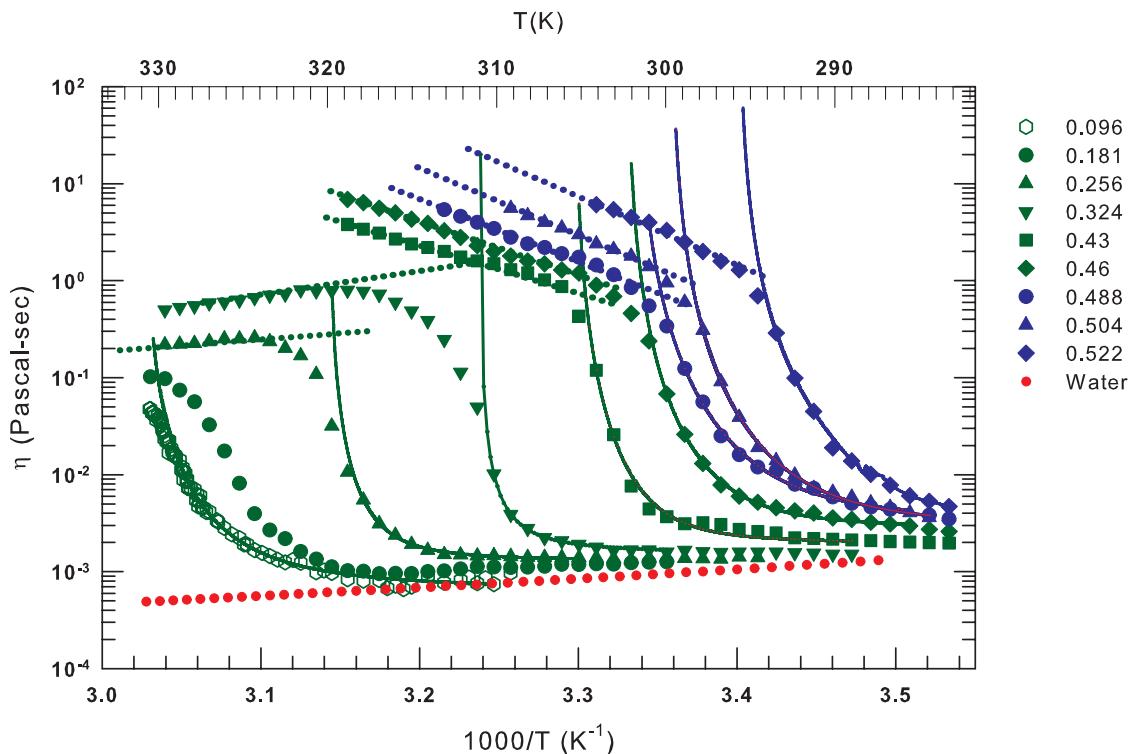
FIG. 5. The log-lin plot, as a function of $1/T$ (bottom axis) and T (top axis), of the viscosities of pure water and of the PL64/D$_2$O AHS micellar system at the following volume fraction: $\phi = 0.096, 0.181, 0.256, 0.324, 0.43, 0.46, 0.488, 0.504$, and 0.522. Open green symbols indicate the critical point volume fraction. Red dots regard the pure water viscosity. The continuous lines represent the data fitting (low T) in terms of the MCT power law (Eq. (1)) with T as the control parameter. The exponent γ ranges from 3.1 to 3.4. The obtained crossover temperatures T_c for each concentration are reported in Fig. 1(a) as large blue circles. Their values can be directly evaluated by means of the Kelvin scale (top axis). For $\phi > 0.256$ can be observed the dynamical crossover from a SA to the exponential AE (dotted lines).
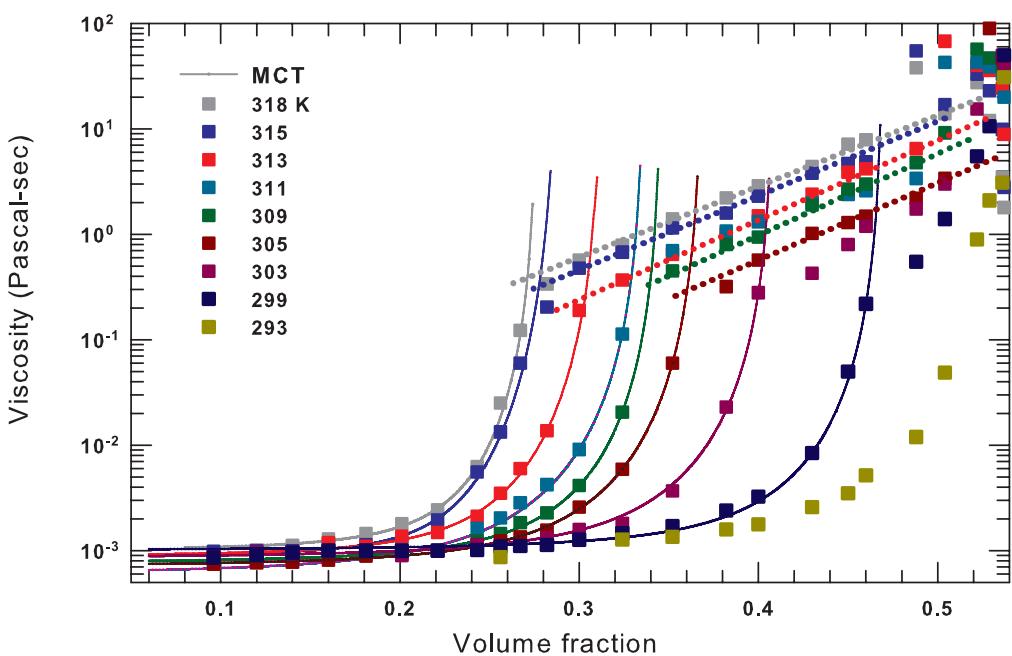

FIG. 6. The PL64/D$_2$O viscosities measured as a function of ϕ for $T = 293, 299, 303, 305, 309, 311, 313, 315$, and 318 K are reported in a log-lin scale. The data are fitted at low ϕ by using the MCT power law (Eq. (1)) with ϕ as the control parameter (continuous line) and the obtained γ values are measured in the interval 3.2 to 3.4. Also in this case is observable, for all the studied temperatures, the dynamical crossover from a strong to fragile glass former behavior, and the corresponding T_c are reported in Fig. 1(a) as large red circles.

critical volume fraction $\phi_c = 0.096$ and the full symbols indicate the other viscosities. The solid lines show the data fitting of the low T data in terms of the MCT power law [Eq. (1)] using temperature T as the control parameter. When $\phi > 0.256$, we see a dynamic crossover from a SA to an exponential AE (dotted lines). This agrees with the behavior seen in the viscosity of the other supercooled liquids[38,43] (Fig. 5). In the Arrhenius region we see that the corresponding activation energy (the $E(T)$, the slope of the dotted lines) changes when ϕ increases. When $\phi = 0.256$ and 0.324, within experimental error $E(T)$ is approximately the same as that of pure water (red dots). When the concentration approaches that of the attractive glass phase $\phi \geq 0.43$, $E(T)$ reverses sign and slowly increases, evolving to an approximate stable value for $\phi > 0.488$. This figure, thus, shows that the overall behavior of $\eta(T)$ as a function of T above percolation when micellar clusters are formed is different for the low and high volume fractions. For low ϕ the activation energy is about the same as that of pure water. The dynamics of the diffusion of a single micellae from one cluster to another is dominated by the solvent viscosity. On approaching the glass phase the situation is very different. Both packing effects and the increase in interparticle interaction (the attraction) changes intercluster diffusion. The decrease in PEO and PPO hydrophilicity is reflected in an increase in T and an increase of the square well depth as T and ϕ increase. Figure 1(a) shows the crossover temperatures (T_c) corresponding to each concentration (large blue circles).

Figure 6 shows a log-linear plot of the viscosities measured as a function of ϕ for $T = 293, 299, 303, 305, 309, 311, 313, 315,$ and 318 K. The data are fit (at low ϕ) by using the MCT power law [Eq. (1)] with ϕ as the control parameter (continuous line). We see a strong-to-fragile dynamic crossover, the dotted lines representing AE behavior, and that when the temperature is decreased the crossover occurs at the higher volume fractions. Figure 1(a) shows the crossover concentration (ϕ_c) obtained for each temperature (large red circles) in terms of the MCT [Eq. (1)]. Both figures confirm that in this AHS system the locus of the dynamic crossover corresponds to the sol-gel (or PT) line where the incipient percolating cluster is formed. This confirms the main prediction of the EMCT, that SA behavior is related to the cage effect but pure AE behavior occurs only after a clustering process produces a structural network capable of supporting hopping. This supports the findings of the NMR data interpreted in terms of a structural crossover in the molecular MSD from pure liquid Brownian behavior to fractal behavior.

In both cases the viscosity exhibits an initial steep growth as the control parameters increase. Scattering data (light and neutron[9,47,48,53]) show that, in this phase diagram region, coalescing clusters of monomers linked by bonds with long lifetimes are formed and, because of this, the viscosity increases by many orders of magnitude, reflecting typical gelation behavior. After a certain threshold this increase ceases and saturation follows. Then the behavior changes and is dominated by cluster deformation or screening effects (due to the finite lifetime of the bonds). As ϕ increases further, the viscosity exhibits a second steep growth until structural arrest is reached. The resulting glass transition can be related to the formation of a spanning cluster made of localized particles connected by bonds. As previously stated, MCT indicates that the presence of bonds is the defining difference between attractive and repulsive glasses. From the data fitting of the SA region (using T and ϕ as control parameters), we find that the exponent γ ranges from approximately 3.1 to 3.4 in both cases, i.e., values analogous to those measured in a similar AHS system, the polystyrene-networked-sphere colloid ($\gamma = 3.6$).[51] In addition, all the calculated T_c values are located just above the system percolation threshold, and the AE region extends from T_c to the dynamic arrest. In summary, the behaviors displayed in the above figures and the results of the scattering experiments confirm the link between clustering and the dynamic crossover that characterizes transport parameters. In contrast, due to cluster polydispersity and the intracluster particle motion of the molecules (micellae in the L64 case), the SA region is related to the onset of the multi-basin energy landscape structure.[18] When clusters form and remain stable for times longer than the molecular bondtime, the only possible motion is hopping. Thus this AHS system, successfully used to test many aspects of the MCT, fully confirms the dynamic crossover explanation provided by EMCT.

V. CONCLUDING REMARKS

We have presented results that help us understand the FS dynamic crossover in an AHS colloidal system (an AHS micellar copolymer) that exhibits strong clustering behavior. We used several experimental techniques, e.g., molecular MSD (NMR) and viscosity measurement, to characterize the system in a wide region of its $T - \phi$ phase diagram. This region includes the disordered liquid phase, the crossing of the percolation line, and the glass phase. Using the viscosity we have explored the phase diagram region that extends from the disordered liquid phase up to the glass transition line. In this examination of viscosity, we have taken into consideration only those data pertaining to the liquid phase above and below the sol-gel transition as we determine how the system approaches dynamic arrest. We have examined in detail the region from the disordered liquid phase to the percolation threshold (PT), and have done this in terms of the ideal MCT power laws [Eq. (1)] by using control parameters T and ϕ to obtain the corresponding critical values T_c and ϕ_c. Above PT the viscosity behavior is purely Arrhenius in both cases. We find that the locus of the measured T_c and ϕ_c in the phase diagram, which defines the dynamical crossover line from a fragile-to-strong glass forming materials, appears to be coincident with the percolation line. In supercooled liquids this crossover is a function of a temperature that is far from the calorimetric glass transition temperature, but in an AHS colloidal system the crossover is also a function of the packing fraction ϕ.

All of these results, taken together, enable us to define two large and distinct phase diagram regions that exhibit contrasting dynamic behaviors, (i) a fragile system exhibiting well-defined super-Arrhenius behavior (described using MCT) that extends from the disordered liquid phase up to the PT line and (ii) a strong glass-forming system that has higher T and ϕ values and that extends from the PT line (also the

locus of the T_c and ϕ_c values) to the glass transition line [see Fig. 1(a)]. In the strong glass-forming system, we observe a region of anomalous "glassy" dynamics beginning before the actual dynamic arrest (the transition from liquid to amorphous solid) at T_c and ϕ_c (also described using MCT). As mentioned above, MCT explains T_c (and hence also ϕ_c) as a singularity resulting from a bifurcation in the self-trapping problem of density fluctuations. We, thus, see two different behaviors above and below these singular values, indicating an important crossover between two different dynamics inside the supercooled liquid phase far from the glass transition. Above T_c the physics is clearly defined by the well-known cage effect, but in the region from T_c (or ϕ_c) to the dynamic arrest we can clarify the dynamic evolution of the glass-forming materials by using the AHS system. We find that the dynamic evolution is dominated by an activated transport process. The T_c and ϕ_c line, thus, defines a real crossover in the physical properties of the glass-forming material. Taking into consideration the particle interactions of the sol-gel transition, we find that structurally these two regions are characterized by a clustering process that starts in the disordered liquid phase and becomes fully developed in the gel phase.[63] In the liquid phase there are many monomers and little polydisperse clusters that increase in size on approaching PT. The NMR experiment indicates that the incipient gel is a self-similar distribution of fractal clusters that range in size from monomers to an infinite cluster. Thus the system dynamics, super Arrhenius in the liquid phase and Arrhenius in the gel phase, are reproduced in the viscosity behaviors.

We have confirmed our results using the MCT framework, more precisely, the EMCT version based on hopping processes. However, the pure liquid phase is described in terms of the classical cage effect. The particle dynamic behavior of the little polydisperse clusters and monomers in this liquid phase is due to a diffusion process in which particles are correlated with each other and do not freely diffuse. If we increase the packing (volume fraction) and the interparticle attractive interactions (temperature), many transport properties change by many orders of magnitude. There is a slowing down, the caging is less effective, and the probability that cage hopping will occur increases. The emerging spanning cluster makes the crossover in the system dynamics possible. Further increases in T and ϕ values impose a new behavior: the only freedom left to the particles is hopping.

In conclusion, our results, i.e., this crossover can be explained as a function of the volume fraction or of the temperature, are based on the MCT model, which can better describe the arrest process in condensed matter than recent empirical approaches.[17] In addition, the FS crossover can be observed using a variable other than temperature, and this supports the hypothesis that the process has universality.

ACKNOWLEDGMENTS

[1] P. G. Debenedetti, *Metastable Liquids: Concepts and Principles* (Princeton University Press, Princeton, 1996).
[2] P. W. Anderson, Science **267**, 1615 (1995).
[3] J. C. Dyre, Rev. Mod. Phys. **78**, 953 (2006).
[4] W. Götze and L. Sjögren, Rep. Prog. Phys. **55**, 241 (1992).
[5] U. Bengtzelius, W. Götze, and A. Sjölander, J. Phys. C **17**, 5915 (1984).
[6] W. van Megen and P. Pusey, Phys. Rev. A **43**, 5429 (1991).
[7] W. van Megen and S. M. Underwood, Phys. Rev. E **49**, 4206 (1994); Phys. Rev. Lett. **70**, 2766 (1993).
[8] L. Fabbian, L. Fabbian, W. Götze, F. Sciortino, P. Tartaglia, and F. Thiery, Phys. Rev. E **59**, R1347 (1999).
[9] S.-H. Chen, W.-R. Chen, and F. Mallamace, Science **300**, 619 (2003).
[10] K. N. Pham, S. U. Egelhaaf, P. N. Pusey, and W. C. K. Poon, Phys. Rev. E **69**, 011503 (2004).
[11] M. L. Williams, R. F. Landel, and J. D. Ferry, J. Am. Chem. Soc. **77**, 3701 (1955).
[12] G. Adams and J. H. Gibbs, J. Chem. Phys. **43**, 139 (1965).
[13] V. Lubchenko and P. G. Wolynes, Annu. Rev. Phys. Chem. **58**, 235 (2007).
[14] D. Kivelson, G. Tarjus, X. Zhao, and S. Kivelson, Phys. Rev. E **53**, 751 (1996).
[15] F. H. Stillinger, J. Chem. Phys. **88**, 7818 (1988).
[16] J. P. Eckmann and I. Procaccia, Phys. Rev. E **78**, 011503 (2008).
[17] V. M. Burlakov and L. Kantorovich, J. Chem. Phys. **134**, 024521 (2011).
[18] F. H. Sitlinger and T. A. Weber, Phys. Rev. A **25**, 978 (1982); Science **225**, 983 (1984).
[19] C. A. Angell, Science **267**, 1924 (1995).
[20] G. P. Johari, Philos. Mag. **86**, 1567 (2006).
[21] G. Tarjus and D. Kivelson, J. Chem. Phys. **103**, 3071 (1995).
[22] M. D. Ediger, Annu. Rev. Phys. Chem. **51**, 99 (2000).
[23] S. F. Swallen, P. A. Bonvallet, R. J. McMahon, and M. D. Ediger, Phys. Rev. Lett. **90**, 015901 (2003).
[24] J. Chang and H. Sillescu, J. Phys. Chem. B **101**, 8794 (1997).
[25] P. Taborek, R. N. Kleinman, and D. J. Bishop, Phys. Rev. B **34**, 1835 (1986).
[26] K. Ito, C. T. Moynihan, and C. A. Angell, Nature (London) **398**, 492 (1999).
[27] F. Mallamace, Proc. Natl. Acad. Sci. U.S.A. **106**, 15097 (2009).
[28] S.-H. Chen, F. Mallamace, C. Y. Mou, M. Broccio, C. Corsaro, A. Faraone, and L. Liu, Proc. Natl. Acad. Sci. U.S.A. **103**, 12974 (2006).
[29] H. E. Stanley, P. Kumar, L. Xu, Z. Yan, M. G. Mazza, S. V. Buldyrev, S.-H. Chen, and F. Mallamace, Physica A **386**, 729–743 (2007).
[30] L. Xu, F. Mallamace, Z. Yan, F. W. Starr, S. V. Buldyrev, and H. E. Stanley, Nat. Phys. **5**, 565–569 (2009).
[31] E. Rössler, K. U. Hess, and V. N. Novikov, J. Non-Cryst. Solids **223**, 207–222 (1998).
[32] R. Richert and C. A. Angell, J. Chem. Phys. **108**, 9016–9026 (1998).
[33] T. Hecksher, A. I. Nielsen, N. B. Olsen, and J. C. Dyre, Nat. Phys. **4**, 737 (2008).
[34] P.-G. de Gennes, *Scaling Concepts in Polymer Physics* (Cornell University Press, Ithaca, 1979).
[35] J. C. Mauro, Y. Yue, A. J. Ellison, P. K. Gupta, and D. C. Allan, Proc. Natl. Acad. Sci. U.S.A. **106**, 19780 (2009).
[36] G. B. McKenna, Nat. Phys. **4**, 673–674 (2008).
[37] J. C. Martinez Garcia, S. J. Rzoska, A. Drozd-Rzoska, and J. Martinez Garcia, Nat. Commun. **4**, 1823 (2013).
[38] F. Mallamace, C. Branca, C. Corsaro, N. Leone, J. Spooren, S. H. Chen, and H. E. Stanley, Proc. Natl. Acad. Sci. U.S.A. **107**, 22457 (2010).
[39] G. Li, W. M. Du, A. Sakai, and H. Z. Cummins, Phys. Rev. A **46**, 3343 (1992).
[40] Y. Yang and K. A. Nelson, J. Chem. Phys. **103**, 7732–7739 (1995).
[41] S. H. Chong, Phys. Rev. E **78**, 041501 (2008).
[42] S. H. Chong, S.-H. Chen, and F. Mallamace, J. Phys.: Condens. Matter **21**, 504101 (2009).
[43] F. Mallamace, C. Corsaro, H. E. Stanley, and S.-H. Chen, Eur. Phys. J. E **34**, 94 (2011).
[44] F. Sciortino and P. Tartaglia, Adv. Phys. **54**, 471–524 (2005).
[45] X. Lu, S. G. J. Mochrie, S. Narayanan, A. R. Sandy, and M. Sprung, Phys. Rev. Lett. **100**, 045701 (2008).

[46] F. Mallamace, P. Gambadauro, N. Micali, P. Tartaglia, C. Liao, and S. H. Chen, Phys. Rev. Lett. **84**, 5431 (2000).

[47] L. Lobry, N. Micali, F. Mallamace, C. Liao, and S. H. Chen, Phys. Rev. E **60**, 7076 (1999).

[48] F. Mallamace, S. H. Chen, Y. C. Liu, L. Lobry, and N. Micali, Physica A **266**, 123 (1999).

[49] F. Mallamace, P. Tartaglia, W. R. Chen, A. Faraone, and S. H. Chen, J. Phys. Condens. Matter **16**, S4975 (2004).

[50] H. Walderhaugh and B. Nyström, J. Phys. Chem. B **101**, 1524–1528 (1997).

[51] E. Bartsch, M. Antonietti, W. Schlupp, and H. Sillescu, J. Chem. Phys. **97**, 3950 (1992).

[52] A. Bartsch, K. Rätzke, A. Meyer, and F. Foupel, Phys. Rev. Lett. **104**, 195901 (2010).

[53] W. R. Chen, S. H. Chen, and F. Mallamace, Phys. Rev. E **66**, 021403 (2002); W. R. Chen, F. Mallamace, C. J. Glinka, E. Fratini, and S. H. Chen, *ibid.* **68**, 041402 (2003).

[54] F. Mallamace, S. H. Chen, A. Coniglio, L. de Arcangelis, E. Del Gado, and A. Fierro, Phys. Rev. E. **73**, 020402 (2006).

[55] K. W. Zhang, B. Lindman, and L. Coppola, Langmuir **11**, 538 (1995).

[56] E. O. Stejskal and J. E. Tanner, J. Chem. Phys. **42**, 288 (1965).

[57] C. Corsaro, J. Spooren, C. Branca, N. Leone, M. Broccio, C. Kim, S. H. Chen, H. E. Stanley, and F. Mallamace, J. Phys. Chem. B **112**, 10449 (2008).

[58] J. Klafter, M. F. Shlesinger, and G. Zumofen, Phys. Today **49**, 33 (1996).

[59] J. P. Bouchaud and A. Georges, Phys. Rep. **195**, 127 (1990).

[60] S. Havlin and D. Ben-Avraham, Adv. Phys. **36**, 695 (1987).

[61] Y. Suzuki and I. Nishio, Phys. Rev. B **45**, 4614 (1992).

[62] A. de Candia, E. Del Gado, A. Fierro, N. Sator, and A. Coniglio, Physica A **358**, 239 (2005).

[63] J. E. Martin, J. Wilcoxon, and J. Odinex, Phys. Rev. A **43**, 858 (1991).